Supplement for Angiotensin-converting enzyme 2 (ACE2) expression increases with age in patients requiring mechanical ventilation.

Steven Andrew Baker M.D. Ph.D.; Shirley Kwok; Gerald J. Berry M.D.; Thomas J. Montine M.D. Ph.D.

This document contains:

Suppl. Methods.

GTEx RNA sequencing analyses. Data for bulk tissue RNA expression level in TPM were downloaded from the portal[1] (GTEx_Analysis_2017-06-05_v8_RNASeQCv1.1.9_gene_tpm.gct). Subject data was acquired from (GTEx_Analysis_v8_Annotations_SubjectPhenotypesDS). Donor age, binned by decade, was treated as a continuous variable and sex as a binary variable. The Hardy scale scores are described by the GTEx consortium[2] as representing the length of the terminal phase culminating in death for each donor with a score of 1 representing a violent and fast death lasting <10 minutes, a score of 2 representing a fast death by natural causes lasting 10 minutes – 1 hour, a score of 3 representing an intermediate rate of death lasting 1 hour – 24 hours, a score of 4 representing a slow death with a terminal phase lasting > 24 hours, and a score of 0 representing donors supported by a ventilator preceding death. A small number of donors in the dataset were not given a Hardy score which is indicated here as unknown. In our linear model the Hardy score was treated as a categorical variable with 6 independent levels (0, 1, 2, 3, 4, and unknown). Thus the β coefficients for each level represent the offset relative to the intercept, β_0, from which *ACE2* expression was regressed on age. A control for tissue ischemic time was performed using data provided in the sample attribute file from the GTEx portal (GTEx_Analysis_v8_Annotations_SampleAttributesDS)[1].

Immunohistochemistry (IHC) staining. Patients were grouped into the ventilated and non-ventilated cohorts based on whether they required mechanical ventilation for AHRF during the admission of and prior to sample collection. Each cohort was stained as a batch. 4µm sections were prepared on SuperFrost Plus slides (Fisher Scientific, cat. # 12-550-15), deparaffinized, and hydrated. Antigen retrieval was carried out in citrate buffer pH 6.0 (Vector Laboratories, cat. # H-3300) at 118°C for 10 minutes. Endogenous peroxidase activity was quenched for 10 minutes in 1% H_2O_2. Sections were blocked in 2.5% normal horse serum (Vector Laboratories, cat. # 30022) and incubated for 1 hour at room temperature with a polyclonal rabbit antibody directed against the human ACE2 C-terminus, aa 788-805 (Abcam, cat. # ab15348) diluted 1:1000 in DAKO Antibody Diluent (Agilent, cat # S0809). After washing, sections were incubated in ImmPRESS Reagent Anti-Rabbit IgG Peroxidase (Vector Laboratories, cat# MP-7401) for 30 minutes at room temperature. Staining was carried out using DAKO Liquid DAB + Substrate Chromogen System (Agilent cat. # K3468) for 1 minute at room temperature. Tissue was counterstained with hematoxylin prior to dehydration and mounting in ClearMount (StatLab cat. # MMC0126). Antibody validation/tittering was performed on normal human kidney and intestine. After identifying the optimal conditions for staining, a sample of these tissues was included alongside our lung samples as a control.

Image Quantification. The DAB signal for each section was extracted via the IHC Toolbox for ImageJ using the default settings for H-DAB. The integrated densities from all 5 fields were summed for each sample and taken as the

total ACE2 signal. These were either compared directly (i.e., normalized by tissue area) or normalized for the total cellularity by quantitating nuclei in the same fields. This was accomplished by extracting the hematoxylin stain using the ImageJ Colour Deconvolution tool utilizing the default vectors for H DAB. An object mask was generated by a custom script (see below) in ImageJ and nuclei counted using the Analyze Particles tool. The total ACE2 signal was divided by the total nuclear count to generate the average ACE2 intensity per cell.

ImageJ Script for nuclei counting.

```
run("Colour Deconvolution", "vectors=[H DAB] hide");
close();
list = getList("window.titles");
    for (i=0; i<list.length; i++){
    winame = list[i];
     selectWindow(winame);
    run("Close");
    }
run("Smooth");
run("Smooth");
run("Smooth");
run("Smooth");
setAutoThreshold("Default");
//run("Threshold...");
setThreshold(0, 160);
run("Close");
//setThreshold(0, 160);
setOption("BlackBackground", false);
run("Convert to Mask");
run("Erode");
run("Erode");
run("Fill Holes");
run("Analyze Particles...", "size=100-2500 show=Outlines exclude include summarize");
close();
close();
```

Macrophage Quantification. Alveolar macrophages were counted by manual pathologist review from the same raw images used for ACE2 quantification and nuclei counting. Total macrophage counts per 5 20x fields of view and total macrophage counts per total number of cells, as measured by the counted nuclei in each image, were plotted using ggplot2 in R.

Suppl. Figure 1. H&E stained images of tissue from main text figures.
Sections were stained from the indicated patients with H&E and representative images collected. The pathological diagnosis for each case is indicated above the image. **A)** The patient presented in Figure 2C showing normal lung parenchyma. **B)** The patients presented in Figure 3 are shown. The left image corresponds to the patient in Figure 3A and reveals restructured airspaces with fibrotic widening of alveolar septa, sparse interstitial inflammation and scattered intra-alveolar macrophages The right image corresponds to the patient in Figure 3B and reveals an acute lung injury pattern with hyaline membranes, prominent AT2 cells lining edematous septa. **C)** The patients presented in Figure 4 are shown. The left image corresponds to the patient in Figure 4A and reveals normal lung parenchyma. The right image corresponds to the patient in Figure 4B and reveals normal lung parenchyma. **D)** The patients presented in Figure 5 are shown. The left image corresponds to the patient in Figure 5A and reveals prominent AT2 cells superimposed on widened fibrotic septa containing chronic inflammatory cell infiltrates. The right image corresponds to the patient in Figure 5B and reveals acute lung injury with hyaline membranes. Scale bars indicate 200μm.

A

23yoF TYPICAL CARCINOID TUMOR, 1.2 CM, EXCISED

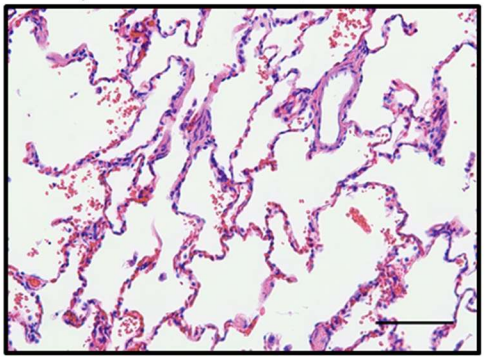

B

67yoM LEFT LUNG, FIBROSING INTERSTITIAL LUNG DISEASE WITH HONEYCOMB CHANGE, ACUTE AND ORGANIZING DIFFUSE ALVEOLAR DAMAGE

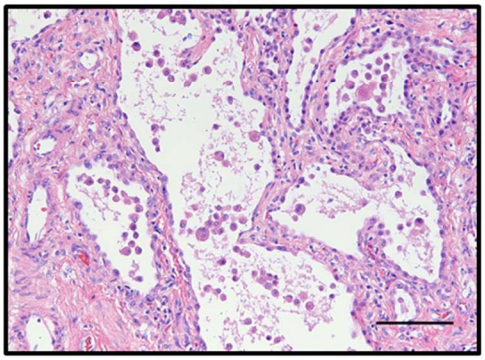

40yoM ACUTE ORGANIZING DIFFUSE ALVEOLAR DAMAGE

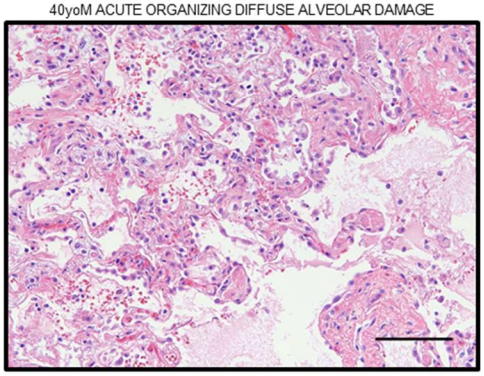

C

77yoM METASTATIC POORLY DIFFERENTIATED ANGIOSARCOMA

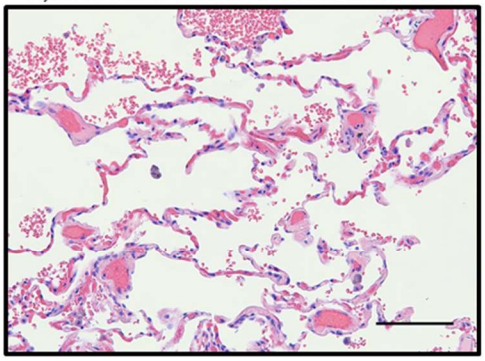

26yoF PLEURAL BLEB AND PATCHY SUBPLEURAL FIBROSIS, CONSISTENT WITH HEALED PNEUMOTHORACES

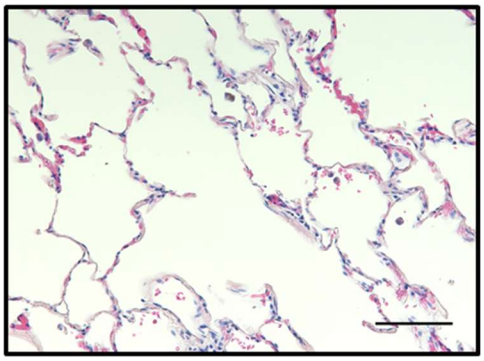

D

83yoM ORGANIZING PHASE OF DIFFUSE ALVEOLAR DAMAGE

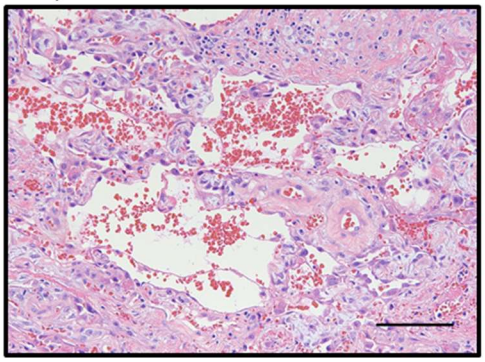

53yoM ACUTE ORGANIZING DIFFUSE ALVEOLAR DAMAGE AND ALVEOLAR HEMORRHAGE SUPERIMPOSED ON FIBROSING INTERSTITIAL LUNG DISEASE WITH USUAL INTERSTITIAL PNEUMONIA (UIP) PATTERN, SECONDARY PULMONARY HYPERTENSIVE CHANGES

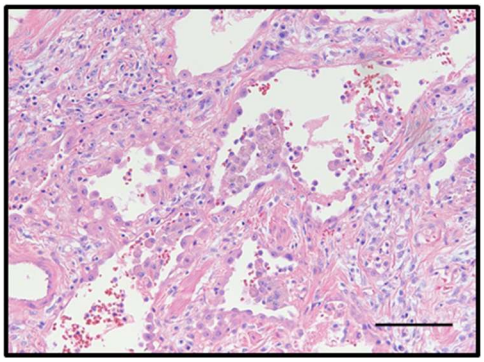

Suppl. Figure 2. Image processing pipeline for ACE2 and cellular quantification.
A) Sections used for quantitative comparison were stained in a single batch and imaged under identical conditions without knowledge of patients' ages. Raw images were processed through an identical pipeline in ImageJ starting with DAB stain extraction using the IHC Toolbox. The histogram was computed for pixel intensity and the integrated density was measured by multiplying the number of pixels by each intensity level. After summing for all 5 20x fields this was taken as the total ACE2 signal. The images shown are taken from the patients presented in Figure 3A and 3B. They reveal the age-related increase in ACE2 seen in the 67yoM on the left compared to the 40yoM on the right. **B)** Cellular counting was performed as described in the Suppl. Methods. A 20x field is shown above and a zoomed-in portion of the same field is shown at each stage in the pipeline below.

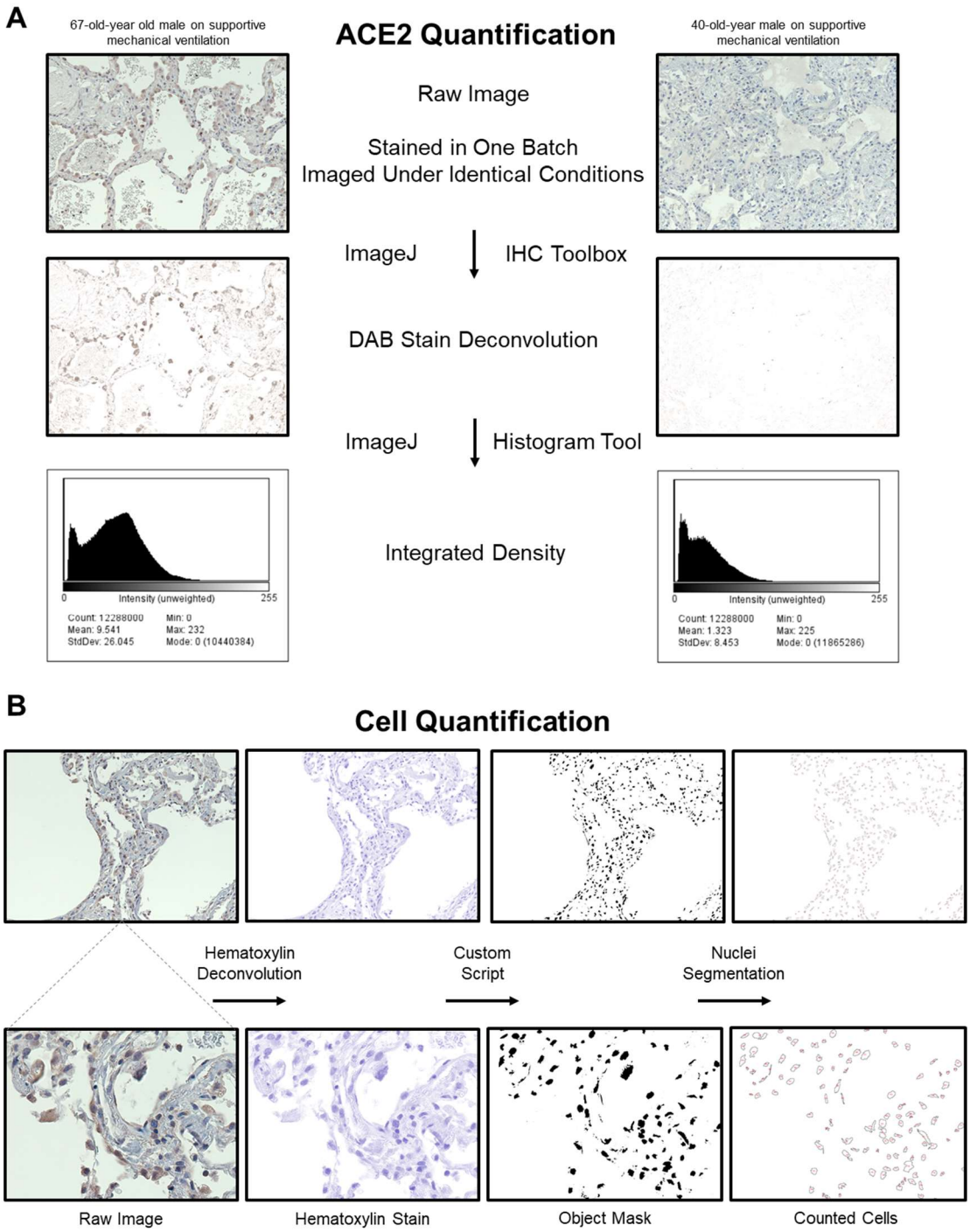

Suppl. Figure 3. Incorporation of sample ischemic time doesn't alter the effect of age on *ACE2* expression. *ACE2* expression in lung stratified by the Hardy scale. Within each Hardy scale group the data are sub-stratified by age. A linear model fit to these data is inset indicating the estimated coefficient for age (β_1) and for ischemic time (β_2) as well as their significance. (n = 26 for a score of 1 representing a violent and fast death lasting <10 minutes, n = 156 for a score of 2 representing a fast death by natural causes lasting 10 minutes – 1 hour, n = 31 for a score of 3 representing an intermediate rate of death lasting 1 hour – 24 hours, n = 64 for a score of 4 representing a slow death with a terminal phase lasting > 24 hours, n = 299 for a score of 0 representing donors supported by a ventilator preceding death, n = 2 with an unknown score). Each point represents a sample from a unique individual. The size of the point indicates the length of ischemic time passed between the death of the donor and sample stabilization scaled as per the legend. Box plots indicate quartiles.

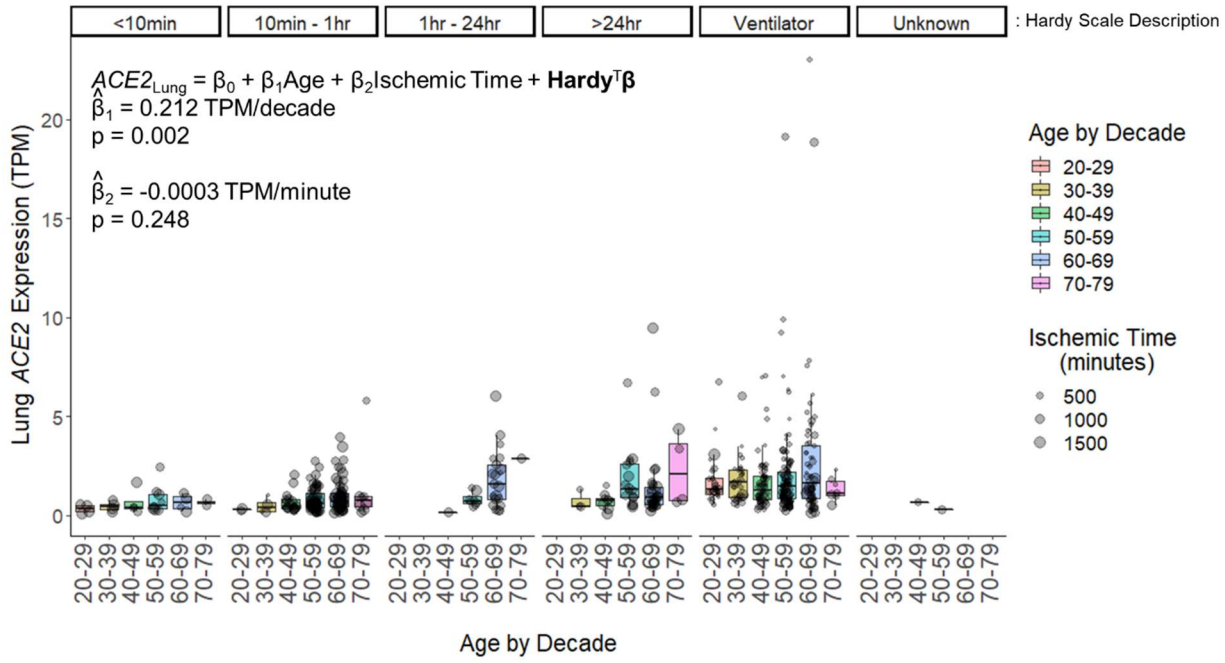

Suppl. Table 1. The relationship of age to tissue *ACE2* expression across the human body.
A linear model was fit for each tissue: $ACE2 = \beta_0 + \beta_1 \text{Age} + \mathbf{Hardy}^T\boldsymbol{\beta}$; predicting *ACE2* expression with age and Hardy score as covariates for each donor contributing a sample. The coefficient for age and its significance is indicated for each tissue type in the GTEx dataset.

Positive Coefficients for Age				**Negative Coefficients for Age**		
Tissue	Coefficient	p value		Tissue	Coefficient	p value
Lung	0.208	0.003		Nerve - Tibial	-0.205	0.0003
Artery - Tibial	0.048	0.013		Whole Blood	-0.003	0.06
Adrenal Gland	0.086	0.02		Cervix - Ectocervix	-0.605	0.069
Liver	0.152	0.021		Minor Salivary Gland	-0.189	0.07
Esophagus - Gastroesophageal Junction	0.2	0.028		Bladder	-0.252	0.08
Esophagus - Muscularis	0.209	0.033		Colon - Transverse	-0.394	0.252
Uterus	0.187	0.041		Pancreas	-0.069	0.336
Muscle - Skeletal	0.056	0.042		Cervix - Endocervix	-0.072	0.384
Fallopian Tube	2.696	0.124		Testis	-0.664	0.44
Thyroid	0.527	0.142		Artery - Aorta	-0.086	0.487
Ovary	1.063	0.142		Brain - Cerebellum	-0.003	0.594
Artery - Coronary	0.449	0.163		Skin - Sun Exposed (Lower leg)	-0.009	0.642
Skin - Not Sun Exposed (Suprapubic)	0.017	0.204		Colon - Sigmoid	-0.053	0.665
Small Intestine - Terminal Ileum	4.357	0.245		Adipose - Visceral (Omentum)	-0.238	0.668
Heart - Atrial Appendage	0.223	0.249		Pituitary	-0.006	0.739
Stomach	0.07	0.282		Prostate	-0.028	0.74
Brain - Nucleus accumbens (basal ganglia)	0.012	0.322		Kidney - Cortex	-0.259	0.8
Brain - Hippocampus	0.017	0.356		Brain - Cerebellar Hemisphere	-0.001	0.838
Breast - Mammary Tissue	0.405	0.358		Adipose - Subcutaneous	-0.027	0.932
Vagina	0.124	0.359		Heart - Left Ventricle	-0.028	0.938
Brain - Hypothalamus	0.011	0.383				
Brain - Caudate (basal ganglia)	0.012	0.395				
Brain - Putamen (basal ganglia)	0.006	0.416				
Brain - Substantia nigra	0.06	0.416				
Brain - Spinal cord (cervical c-1)	0.014	0.48				
Cells - EBV-transformed lymphocytes	0.001	0.61				
Brain - Cortex	0.004	0.633				
Brain - Anterior cingulate cortex (BA24)	0.004	0.738				
Cells - Cultured fibroblasts	0.002	0.822				
Brain - Amygdala	0.002	0.838				
Spleen	0.001	0.873				
Brain - Frontal Cortex (BA9)	0.002	0.899				
Esophagus - Mucosa	0.009	0.899				

Suppl. Figure 4. Mouse scRNAseq indicating which lung cell types express detectable *Ace2*.
Droplet sequencing data from the Tabula Muris portal were imported into R and the percentages of each cell type in lung with non-zero counts for *Ace2* were plotted. Type II Pneumocytes (AT2 cells) exhibit the highest fraction of detectable *Ace2* expression.

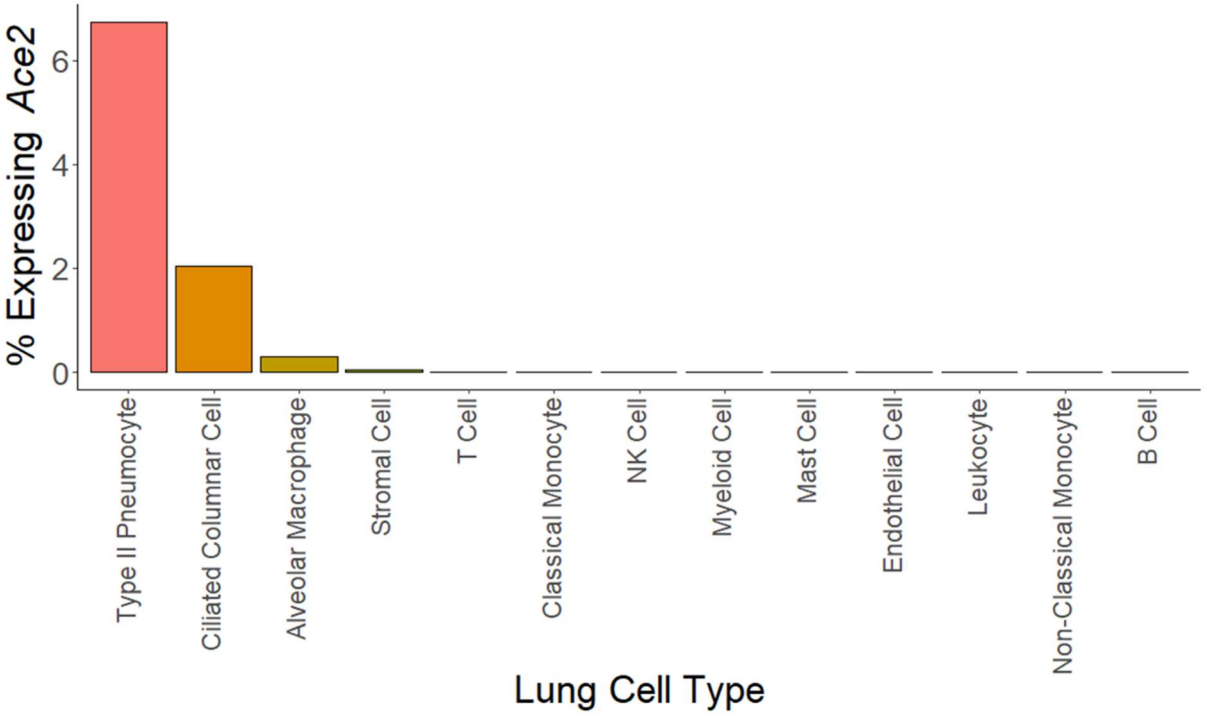

Suppl. Table 2. Patient information for lung cases used in this study.
The patient age, sex, ventilatory status, prescription information for ACEI/ARB therapy, and pathological diagnosis are given for each sample used. The * denotes the 67yoM sampled for a double lung explant whose tissue was also used as a control for staining/measurement reproducibility as described in the Results section of the main text.

Age	Sex	Supportive Ventilation	ACEI/ARB	Pathological Diagnosis
62	F	Yes	No	DIFFUSE ALVEOLAR DAMAGE
62	M	Yes	No	USUAL INTERSTITIAL PNEUMONIA, ORGANIZING PHASE DIFFUSE ALVEOLAR DAMAGE
53	M	Yes	No	ACUTE AND ORGANIZING DIFFUSE ALVEOLAR DAMAGE SUPERIMPOSED ON USUAL INTERSTITIAL PNEUMONIA
51	M	Yes	No	ORGANIZING PHASE OF DIFFUSE ALVEOLAR DAMAGE
*67	M	Yes	No	LEFT LUNG, FIBROSING INTERSTITIAL LUNG DISEASE WITH HONEYCOMB CHANGE, ACUTE AND ORGANIZING DIFFUSE ALVEOLAR DAMAGE
*67	M	Yes	No	RIGHT LUNG, FIBROSING INTERSTITIAL LUNG DISEASE WITH HONEYCOMB CHANGE, ACUTE AND ORGANIZING DIFFUSE ALVEOLAR DAMAGE
40	M	Yes	No	ACUTE ORGANIZING DIFFUSE ALVEOLAR DAMAGE
57	F	Yes	No	DIFFUSE ALVEOLAR DAMAGE, ORGANIZING PHASE
83	M	Yes	Valsartan 160mg bid	ORGANIZING PHASE OF DIFFUSE ALVEOLAR DAMAGE
47	M	Yes	No	FIBROSING INTERSTITIAL LUNG DISEASE WITH SUPERIMPOSED ACUTE AND ORGANIZING DIFFUSE ALVEOLAR DAMAGE
53	M	Yes	Lisinopril 5mg qd	ACUTE ORGANIZING DIFFUSE ALVEOLAR DAMAGE AND ALVEOLAR HEMORRHAGE SUPERIMPOSED ON FIBROSING INTERSTITIAL LUNG DISEASE WITH USUAL INTERSTITIAL PNEUMONIA (UIP) PATTERN, SECONDARY PULMONARY HYPERTENSIVE CHANGES
40	F	Yes	No	ORGANIZING DIFFUSE ALVEOLAR DAMAGE
14	M	No	No	BLEB, SUBPLEURAL FIBROSIS
18	M	No	No	PLEURAL BLEB AND SUBPLEURAL FIBROSIS
15	F	No	No	ALVEOLATED LUNG PAREANCHYMA WITH BLEB FORMATION, SUBPLEURAL FIBROSIS AND REACTIVE CHANGES
77	M	No	No	METASTATIC POORLY DIFFERENTIATED ANGIOSARCOMA
24	M	No	No	PLEURAL BLEB
23	F	No	No	TYPICAL CARCINOID TUMOR, 1.2 CM, EXCISED
68	F	No	No	METASTATIC ADENOCARCINOMA CONSISTENT WITH COLORECTAL ORIGIN, 1.4 CM, EXCISED
18	M	No	No	PLEURAL BLEB
26	F	No	No	PLEURAL BLEB AND PATCHY SUBPLEURAL FIBROSIS, CONSISTENT WITH HEALED PNEUMOTHORACES
75	M	No	No	METASTATIC NASOPHARYNGEAL CARCINOMA
33	M	No	No	METASTATIC ADENOCARCINOMA, CONSISTENT WITH COLORECTAL ORIGIN, EXCISED
20	M	No	No	METASTATIC OSTEOSARCOMA, 1.7 CM, EXCISED
31	F	No	No	LUNG PARENCHYMA WITH PLEURAL BLEB FORMATION
58	F	No	No	INVOLVED BY LEIOMYOSARCOMA
70	F	No	No	TWO FOCI OF METASTATIC COLORECTAL ADENOCARCINOMA, EXCISED
30	M	No	No	PLEURAL BLEB; EXCISED

80	F	No	No	METASTATIC MALIGNANT PHYLLODES TUMOR, 3.0 CM, EXCISED
56	M	No	No	METASTATIC COLORECTAL ADENOCARCINOMA, 1.0 CM; EXCISED
46	F	No	No	METASTATIC COLORECTAL ADENOCARCINOMA; 1.1 CM; EXCISED
49	F	No	No	HIGH GRADE MALIGNANT NEOPLASM CONSISTENT WITH METASTATIC MALIGNANT PHYLLODES TUMOR; 1.6 CM; EXCISED
*Note: this patient had two lung specimens collected at the same time (one form the left lung and one from the right lung with similar findings as indicated in the pathological diagnoses)				

Suppl. Figure 5. The abundance of alveolar macrophages does not change with age in ventilated patients. **A)** Visual counting of alveolar macrophages was carried out on samples from ventilated patients (n = 12 samples from 11 patients). The total number of alveolar macrophages from 5 low power fields is plotted relative to the patient's age at the time of specimen collection. A linear fit to the data is indicated by the dashed line with the 95% confidence interval highlighted in grey. **B)** The same specimens quantitated in (A) were normalized by cellularity and the number of alveolar macrophages divided by the total cell count is plotted along with a linear fit to the data and its 95% confidence interval.

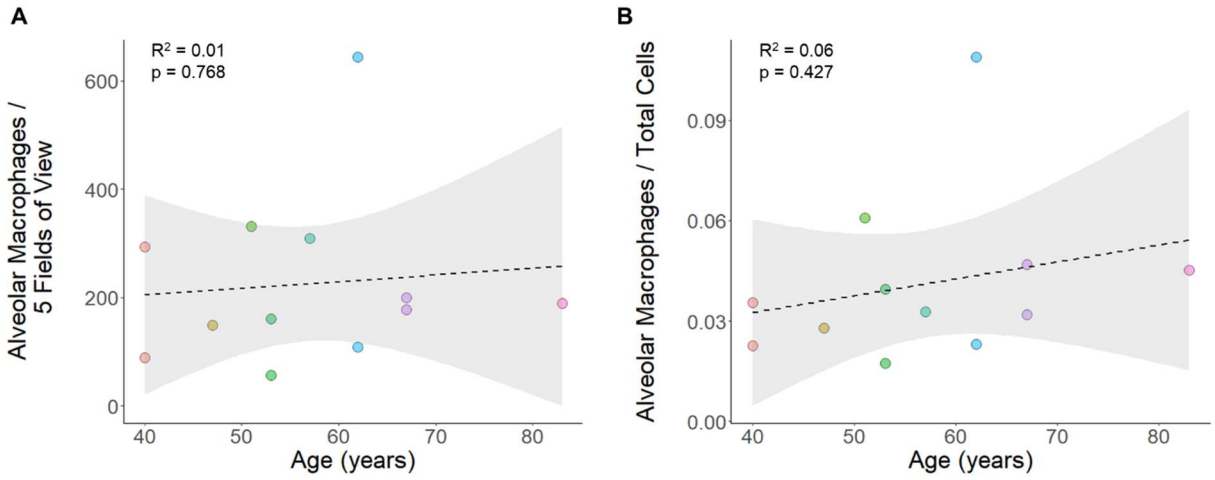

Suppl. References.

1. GTEx Consortium. GTEx Portal. Accessed April 22, 2020. https://www.gtexportal.org/home/

2. GTEx Consortium. Hardy scale description. Accessed June 5, 2020. https://www.ncbi.nlm.nih.gov/projects/gap/cgi-bin/variable.cgi?study_id=phs000424.v4.p1&phv=169092#:~:text=Death%20classification%20based%20on%20the,phase%20estimated%20at%20%3C%2010%20min.